SLAC – PUB – 3944
April 1986
A

SPECIAL SLC LINAC DEVELOPMENTS*

JOHN T. SEEMAN and JOHN C. SHEPPARD
Stanford Linear Accelerator Center, Stanford, California 94305

1. Summary

The linac of the SLAC Linear Collider (SLC) is required to accelerate several intense electron and positron bunches to high energy while maintaining their small transverse dimensions and energy spectra. Many of the linac systems have been upgraded to the new stringent SLC design criteria. The remaining systems will be completed in the summer of 1986. Special instruments and controls have been developed to monitor and manipulate these small but potent beams. A brief review of the SLC requirements is given. A broad survey of the recent developments is made encompassing longitudinal and transverse wakefield reductions, Landau damping, energy and position feedback systems, beam diagnostics and beam current fluctuations.

2. Linac Overview and Goals

A schematic of the SLC linac is shown in Fig. 1. The linac downstream of the damping rings has a length of 2946 m and is powered by 229 klystrons. The accelerating gradient is about 18 MV/m. A strong focusing FODO lattice consisting of 282 quadrupoles is used to control the transverse beam size. A pair of $x - y$ correction dipoles and a stripline position monitor are associated with each quadrupole. Several high resolution profile monitors and wire scanners are located along the linac to measure the beam sizes. Energy, energy spectrum, and emittance enlargement monitors are placed near the end of the linac to allow automatic feedback during SLC operations.

The primary goal of the linac is to transform the six dimensional phase space volume of a low emittance, low energy beam to high energy without significant phase space enlargement. Table 1 lists the parameters of both beams as they enter and exit the linac. The phase space volume can be represented by a product of the six beam dimensions assuming upright ellipses.

$$\text{Vol} = \sigma_E \cdot \sigma_z \cdot \sigma_x \cdot \sigma_{x'} \cdot \sigma_y \cdot \sigma_{y'} \quad ,$$

where σ_E is the beam energy spread, σ_z the bunch length, and $\sigma_{x(x')}$ and $\sigma_{y(y')}$ the horizontal and vertical transverse position and angular sizes. SLC studies[1,2] indicate that the presently planned transverse wakefield control and feedback should limit the increases in the transverse dimensions to small values. The bunch length remains constant by virtue of the relativistic particle velocities. The absolute energy width, however, increases about a factor of twelve because of the longitudinal wakefields and the finite bunch length. The relative energy spread, σ_E/E, is more important and, fortunately, decreases by a factor of four.

Table 1. SLC Linac Beam Parameters

Location	Entrance	Exit
Energy (GeV)	1.21	50.
Energy Spread (%)	0.7	0.2
Bunch Length (mm)	1.5	1.5
Inv. Emittance ($\times 10^{-5}$ r-m)	3.0	3.0
Maximum Beam Size (μm)	356	129
Minimum Beam Divergence (μrad)	36	2.5
Peak Betatron Function (m)	10	55
Average Betatron Function (m)	6	38

3. Longitudinal Phase Space

ACCELERATION:

The beams are accelerated to high energy using klystrons operating with SLED.[3,4] The power from each klystron is divided amongst four ten-foot accelerator sections. Because of beam loading, wakefield compensation and radiation in the ARCs, each forty foot 'girder' must provide 252 MeV of available acceleration so that two bunches can arrive at the interaction region each with an energy of 50 GeV. The klystrons are operated with different modulator pulse lengths. The SLED gain multiplier and required klystron output power required for 252 MeV are plotted against pulse length in Fig. 2. Originally, the klystron was designed to make 50 MW with a 5.0 μsec pulse width. Recent tests have shown that 67 MW-3.5 μsec operation is more efficient.

The acceleration of a bunch with respect to the timing of that bunch on the SLED gain curve is shown in Fig. 3. The curvature of the SLED energy gain with time allows the ratio of the positron to electron energies to be adjusted.

The phase and amplitude of each klystron is monitored and adjusted using a new control system[4,5] designed to maintain the SLC phase and power tolerances of about 0.2° and 0.2%, respectively. Equipment is being designed to monitor the output of each klystron on every pulse and report to the feedback systems out-of-tolerance pulses.

The energy spectrum of an SLC beam is determined by the length and intensity of the bunch and RF parameters. Bunch lengths produced by the damping ring complex are in the range of 0.5 to 1.5 mm. At high bunch intensities,

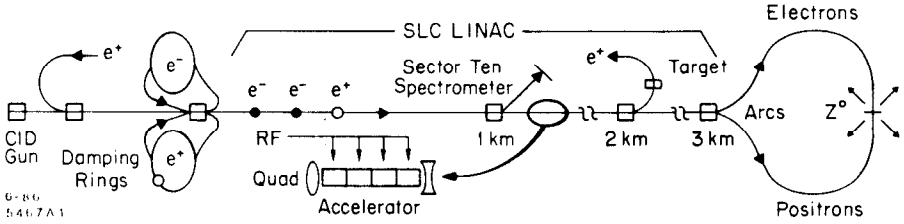

Fig. 1. Schematic of the SLC Linac and Adjoining SLC Components

*Work supported by the Department of Energy, contract DE–AC03–76SF00515.

Invited talk presented at the Stanford Linear Accelerator Conference, Stanford, California, June 2-6, 1986

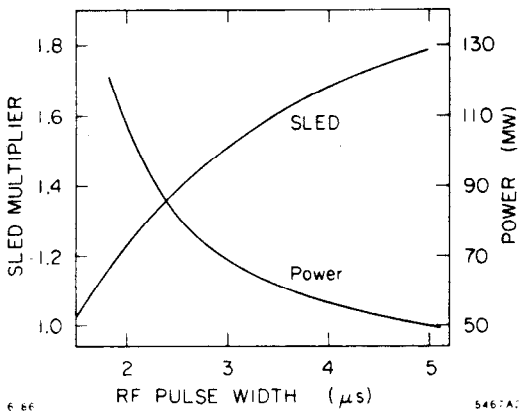

Fig. 2. SLED multiplier and required klystron output power to produce 252 MeV energy gain versus pulse width.

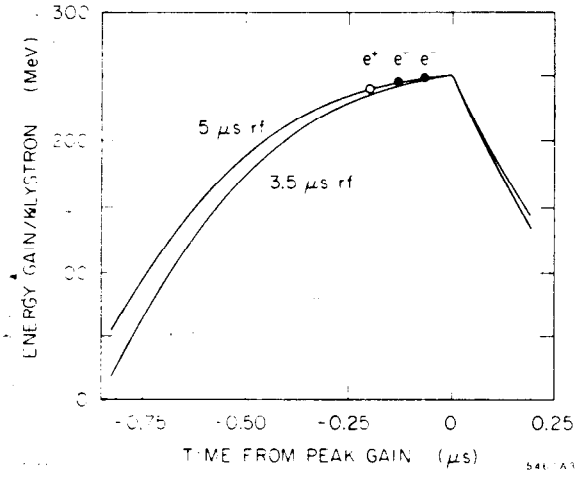

Fig. 3. Energy gain versus bunch arrival time with SLED.

strong intrabunch longitudinal wakefields[6] cause position dependent deceleration within the bunch. For example, at 5×10^{10}, the tail will be decelerated about 2 GeV. To compensate, the RF phase is adjusted so that the bunch is centered ahead of the voltage crest where the RF gradient nearly cancels the wakefield induced gradient. Two simulated energy spectra representing high and low bunch intensities are shown in Fig. 4. Both spectra have widths less than 0.2% RMS when 1% energy cuts are made. The shape difference between the two plots is quite striking and represents the influence of the longitudinal wakefields. The particles that are far off-energy are due to the nonlinear nature of the RF and wakefield forces and are removed from the beam early in the ARCs by momentum defining slits. Radiation in the ARC bending magnets will further broaden the spectra of Fig. 4 by about 0.08% before the bunch arrives at the final focus.[7]

The energy spectrum at the end of the linac is affected by the length of the bunch. At low currents the energy spectrum is minimized with short bunches because the longitudinal wakefields are very weak and the curvature of the RF sine wave is minimized. At high intensities longer bunches allow the greater curvature of the RF to compensate for the strong wakefield effects. The optimum bunch length to minimize the energy spectrum versus bunch intensity is shown in Fig. 5.

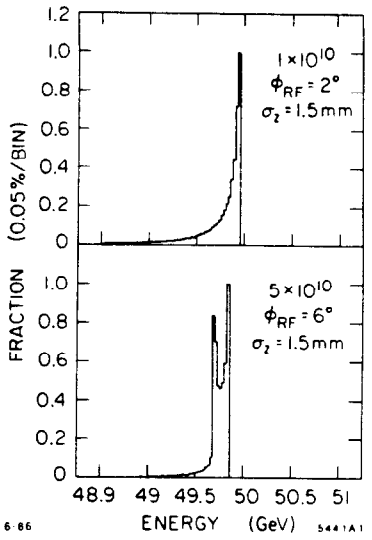

Fig. 4. Expected energy spectra at two beam intensities.

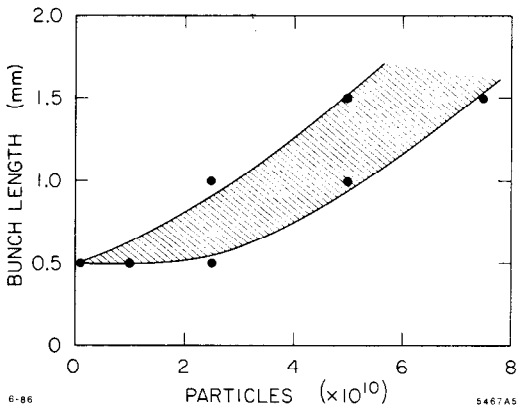

Fig. 5. Optimum bunch length as a function of bunch intensity to minimize the energy spectrum.

ENERGY AND ENERGY SPECTRUM FEEDBACK:

The energies and energy spectra of the e^+ and e^- beams will be monitored after the splitter dipole magnet at the end of the linac (beginning of the ARCs) in a special location where the dispersion induced beam size dominates the betatron size of the beam. The energy of each beam will be measured using stripline position monitors.[8] Each energy spectrum will be measured using a nondisruptive synchrotron radiation monitor incorporating a half-wavelength vertical wiggler and an off-axis x ray position detector.[9] These four signals will be monitored and processed by a stand-alone microcomputer. Correction signals will be calculated and broadcast, ultimately at 120 Hz, to four controls using a dedicated channel on the computer communications cable. The bunch phases in the two damping rings, the RF amplitude of the linac klystrons (adjusted by making opposing changes in the phases of two sectors of eight klystrons each), and the timing of the bunches on the SLED gain curve are the control variables. An overview of the feedback system is shown in Fig. 6 and a list of the nominal control values are included in Table 2.

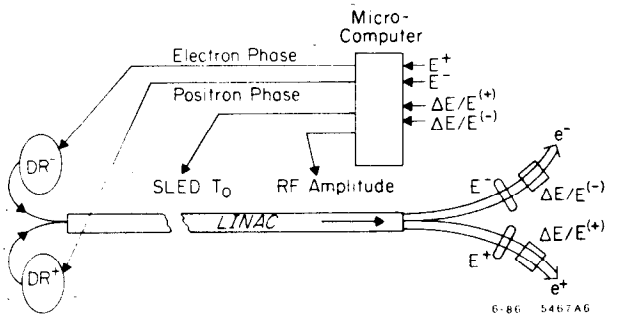

Fig. 6. Overview of the energy and energy spectrum feedback system.

Table 2.

SLC energy parameters for 48 GeV per beam at the IP and 49.3 GeV at the end of the linac. SLED timing is for the positron bunch before the peak SLED gain (Fig. 3).

Case	A	B	C	D	E	F
$N(e^- \times 10^{10})$	5	5	1	5	5	1
$N(e^+ \times 10^{10})$	5	1	1	5	1	1
σ_z (mm)	1.5	1.5	1.5	1.0	1.0	1.0
ϕ_{RF} (e^-) (deg)	6	6	2	10	10	2
ϕ_{RF} (e^+) (deg)	6	2	2	10	2	2
Klystrons (#)	201.7	203.6	192.7	204.6	216.6	192.9
SLED Timing (ns)	-131	-201	-57	-130	-294	-57

RECOVERY FROM BEAM INTENSITY FLUCTUATIONS:

From time to time the SLC will experience single pulse losses of one (or both) beam(s). The linac was designed to allow for automatic recovery to nominal conditions except at very high bunch intensities. The problems arise from longitudinal beam loading of the bunches on themselves and on following bunches. Changes in bunch currents can move the energies of that bunch and subsequent bunches beyond the finite energy acceptances of the damping rings (± 1% of 1.2 GeV) and the electron extraction line for positrons (± 2% of 33 GeV).

In the linac upstream of the damping rings, the electron bunches are ahead of the positron bunch. A missing positron bunch will not affect the electron bunches. Those electrons will generate more positrons and repopulate the SLC. Missing electron bunches cause the positron bunch to be lost also. However, new electron bunches alone can restart the SLC, as mentioned above.

This recovery problem for the 33 GeV electron extraction line required a different solution because the ARCs and Final Focus were designed assuming the positron bunch came first. Fortunately, a missing positron bunch at 5×10^{10} particles causes the second, scavenger, electron bunch only to lose about 25% of its intensity on the extraction line aperture. This allows most of the new positrons to be made and recovery to full intensity occurs in a few pulses. For positron bunch intensities above about 6×10^{10} a single missing pulse will cause the scavenger e^- bunch to be totally lost on the aperture requiring a careful bootstrap procedure. Missing electron bunches will stop the positron production. Both will recover together when the electron bunches return.

4. Transverse Phase Space

TRANSVERSE WAKEFIELDS:

A particle bunch executing betatrons oscillations down the linac or passing through a misaligned accelerating section will experience transverse wakefield forces. These forces are due to asymmetric fields generated by off-axis particles. These forces deflect trailing particles depending on their longitudinal positions. The wakefields for the SLAC structure were calculated several years ago[6] and analytic methods for calculating their effects for the SLC were developed.[10] The results of some tracking simulations are shown here to indicate how the linac was modified to minimize transverse wakefield effects.

Many of the important parameters can be seen by examining expressions for the transverse motion x of the head of the bunch, the angular deflection given to the tail of the bunch θ_W by transverse wakefields, and the relative ratio of the deflection to the natural beam divergence angle $\theta_{x'}$.

$$x(z) = x_0 \, [\beta(z)/\gamma(z)]^{1/2} \, \sin[2\pi z/\lambda(z)] \quad ,$$

$$\theta_W(z) \propto x(z)/\gamma(z) \quad ,$$

and

$$\theta_W(z)/\theta_{x'} \propto [x_0\beta(z)/\gamma(z)] \, \sin[2\pi z/\lambda(z)] \quad .$$

x_0 is the initial offset, β the betatron function, $\gamma = E/m_0c^2$, λ the local betatron wavelength and z the position along the linac. Clearly, the deflection can be minimized compared to the natural divergence angle by limiting the injection offset, accelerating as rapidly as possible, and reducing $\beta(z)$.

LINAC LATTICE:

Periodic drift sections in the original SLAC linac occur every 12.3 m. Two styles of quadrupoles have been placed in these drifts, type QE and type QC. The QE magnets have a gradient length of 106 kG and are placed in the first 300 meters and the last 2000 meters of the linac. The QC magnets have a strength of 87 kG and occupy the central 600 meters. Beam position monitors have been placed in the bore of each quadrupole and a pair of dipoles placed nearby allow precise $x - y$ orbit correction,[11,12] to below 100 μm (RMS) for two beams.

Two years ago a program was approved to reduce the betatron function in the first 300 meters of linac downstream of the damping ring. This program reduced the quadrupole spacing and betatron function a factor of four in the first 100 m and a factor of two in the next 200 m. The reduction allowed the tolerances on injection errors to increase about a factor of two. To make space for the new quadrupoles, accelerator sections were removed from the linac and five cells were carefully cut out. The sections were rebrazed, RF tuned, vacuum baked and reinstalled. Forty-three accelerator sections were shortened. High power RF tests at 50 MW have not shown any problems.

The resulting lattice is shown in Fig. 7. The betatron function on the right is indicative of the remainder of the linac. The phase shift per cell is about 90 degrees for the first 1500 m. Whereafter, the quadrupoles are held at their saturated strengths and the phase shift per cell decreases slowly to about 42° at the end of the linac.

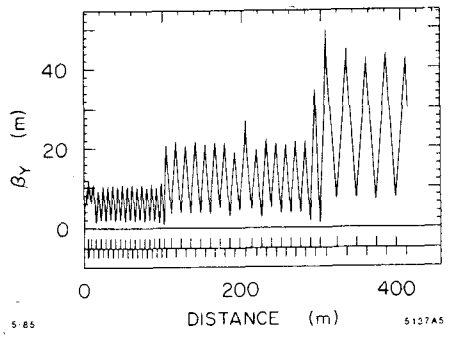

Fig. 7. Typical linac vertical betatron function.

EFFECTS OF BETATRON OSCILLATIONS:

If a particle is launched into the linac with an error in angle or position relative to the accelerator axis, then the transverse wakefields produced by the longitudinal charge distribution will resonantly drive the particles following the bunch head to ever increasing amplitudes. The integrated transverse size of the bunch grows and the effective emittance increases. This transverse enlargement has been observed in the linac during the Ten Sector Tests.[1,2] An example is shown in Fig. 8, where a low emittance beam from the damping ring is reinjected and viewed on a profile monitor 1000 m downstream in the linac. The left photograph shows a beam which is properly aligned in the linac and shows no enlargement. Its full width at half maximum is about 300 microns. The photograph on the right shows the same beam except it was made to perform a 1 mm betatron oscillation along the linac. The head of the bunch is at the top of the picture and the tail extends downward about 1 mm. Results of tracking simulations with these beam conditions are not inconsistent with these data. Video signals similar to these photographs from profile monitors at the end of the linac will be digitized[13] and used as input signals to the transverse feedback system (described below).

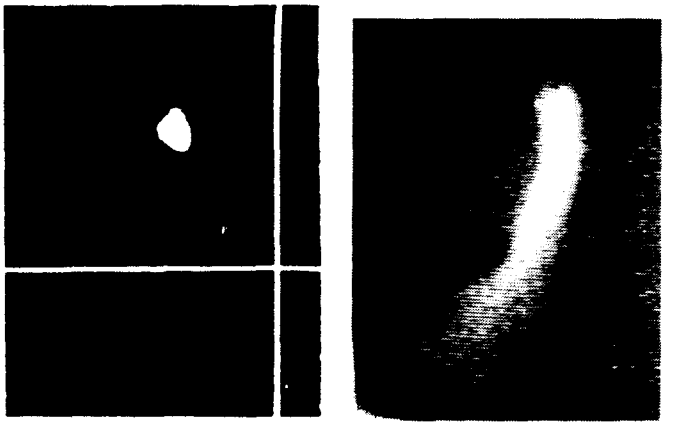

Fig. 8. Photographs of a reinjected damping ring beam in the linac with and without a 1 mm betatron oscillation. The bunch contained 5×10^9 electrons at 6.8 GeV. The tail (about 1 mm long) was generated by transverse wakefields.

LANDAU DAMPING:

The reason transverse wakefields are so limiting is that all particles in the beam oscillate at the same frequency, leading to resonant excitation. Landau damping is a technique which separates the oscillation frequencies of the particles in the beam by introducing a longitudinal energy spread along the bunch. This is produced by back phasing early klystrons and forward phasing later klystrons, ultimately keeping the energy spectrum small at the entrance to the ARCs. This technique has been studied by many people, *e.g.*, Refs. 14 and 15. Landau damping has many selectable variables such as the total energy lost, how rapidly the energy spread is introduced and removed, and the positioning of the amplitude beats at the end of the linac. One example of the energy spread introduced in a bunch of 5×10^{10} particles at various points in the SLC linac is shown in Fig. 9. The first 24 klystrons have a phase of -30° and the remainder +16°. This phase distribution is used in all of the following discussions employing Landau damping.

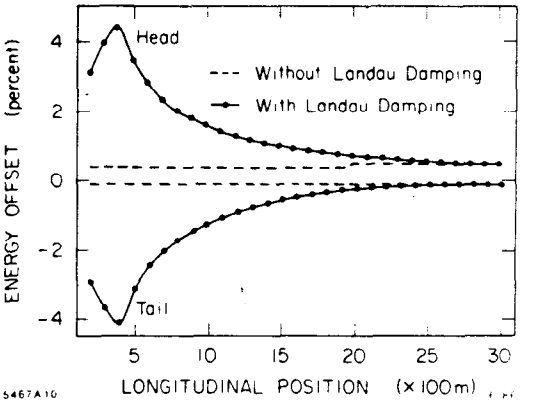

Fig. 9. Induced energy spread in the beam using Landau damping.

INJECTION TOLERANCES:

Static injection errors in launch position or angle into the linac can be corrected by static dipole corrections. However, varying components which deflect the beams (for example, unstable dipole power supplies, vibrating quadrupoles, or unstable klystrons which produce RF deflections) must be carefully controlled or eliminated. Acceptable tolerances can be calculated using tracking programs. These programs incorporate the linac FODO lattice, transverse and longitudinal wakefields, RF acceleration, and gaussian weighted charge distributions. The RF phases are always chosen to produce a 0.2% energy spectra at the end of the linac. A convenient measure of the tolerance is the value of the injection error at which the centroid of the particles about 1 mm behind the bunch center is elevated to a phase space position corresponding to the nominal emittance of the injected beam. The corresponding loss in luminosity is about 10%. Figure 10 shows the calculated tolerance in the injection position as a function of bunch intensity. The tolerance falls about three orders of magnitude over the operating intensity range of the SLC. Landau damping improves the tolerances about a factor of ten.

The transverse wakefields vary roughly linearly with the bunch length.[6] This fact is apparent in the simulations, as can be seen in the plot of Fig. 11 where the tolerances increase as the bunch length decreases. Some care must be taken when interpreting these data because the nature of the bunch enlargement is bunch length dependent and recording only the results from one position in the bunch may mask additional considerations.

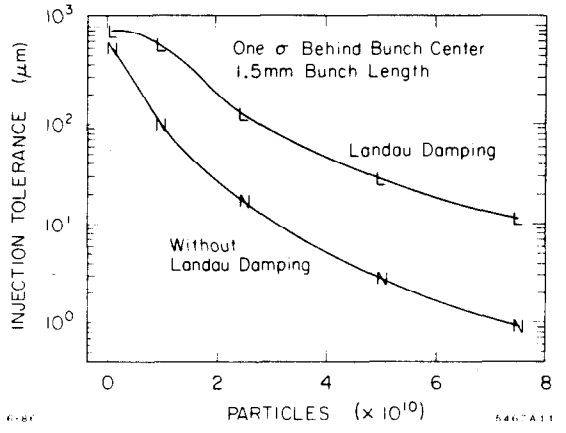

Fig. 10. Maximum injection tolerance vs bunch intensity.

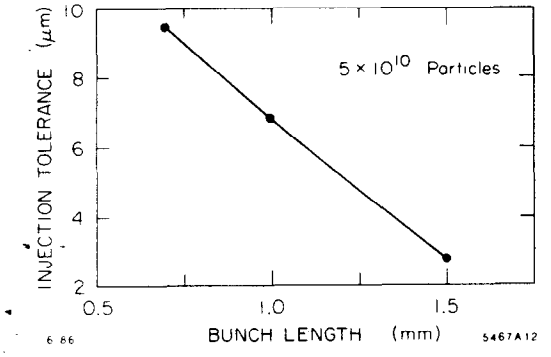

Fig. 11. Injection tolerance vs bunch length.

LIMITS ON RESIDUAL DISPERSION AT THE LINAC ENTRANCE

The dispersion function η experienced by the beam as it enters the linac can be determined by extending η from the damping ring through the adjoining transport line (RTL). The transport line is designed to shorten the bunch longitudinally using an accelerating cavity and a tailored η function. If the damping ring–RTL complex is not tuned properly, dispersion will be present in the beam at the entrance to the linac where a value of zero is expected. A residual dispersion affects the SLC beam in two ways. The first is intensity independent and increases the apparent emittance of the beam by widening the bunch. Calculations[16] indicate that η must be kept below about 13 mm at the linac entrance (β = 6.6 m) so that no detrimental size increase occurs. An associated limit on η' can also be calculated.

The second effect includes the linac wakefields. With a residual dispersion and a partially compressed bunch (presently the SLC design), the particles entering the linac will have correlations between their longitudinal and transverse positions, which will lead to transverse wakefield enlargement. This effect can be visualized by reviewing the compression process[17] shown in Fig. 12. With full compression the head, tail and center particles have the same longitudinal position at the linac entrance and the bunch length is at a minimum (about 0.5 mm). If the compression voltage is lowered, then the bunch is not fully compressed and a longitudinal position–energy correlation exists. The present SLC design calls for a bunch length of 1.0 to 1.5 mm. If a residual dispersion is present in the beam at the linac entrance, then a longitudinal-transverse position correlation results.

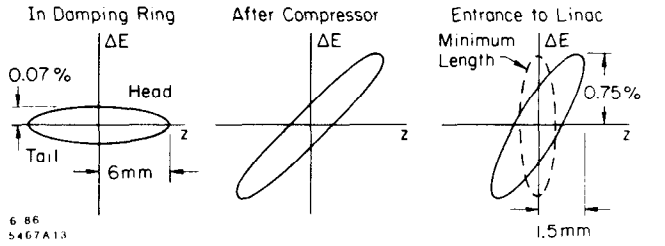

Fig. 12. Compression of the damping ring beam showing longitudinal position – energy correlations at the linac entrance. Residual dispersion η and these correlations cause linac wakefield effects.

Simulations[18] have been made to predict the effects of these correlations and the results are shown in Fig. 13. The allowed dispersion is highly current dependent because the wakefields are nonlinear with the bunch intensity. Without Landau damping, the limits become quite small at high currents, even exceeding those required for the final focus. If in addition carefully chosen injection offsets are used which place the bunch head near the accelerator axis, then the tolerances can be relaxed by a factor of three to six. Finally, Landau damping also has a strong effect on the tolerances of residual dispersion. Landau damping deliberately introduces longitudinal position-energy correlations into the beam which in the presence of injection position and angle errors produces longitudinal-transverse position correlations in a bunch at many locations along the linac. It is then not surprising that Landau damping and injection offsets and angles can be used to compensate the dispersion induced correlations and raise the limits on residual dispersion. The drawbacks are that Landau damping requires extra acceleration from the RF system and very sizable offsets and angles are required.

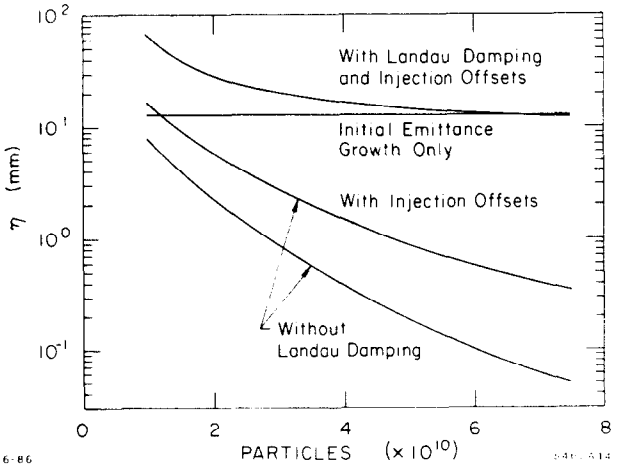

Fig. 13. Allowed dispersion vs beam intensity at the entrance to the linac, as limited by transverse wakefields. Criteria identical to those of Fig. 10 have been used.

TRANSVERSE RF DEFLECTIONS:

Small asymmetries in an accelerating structure produce transverse fields that deflect beams. For the SLC these deflections are in the same direction for both e^+ and e^- beams, and can only be corrected by special 'magic' dipole bumps[19]. If a klystron is unstable, then the varying deflections will cause the beams to jitter. Thus, the size of the structure asymmetries place corresponding limits on the stability of the klystrons.

Studies of the SLAC structure have found three asymmetries. The horizontal asymmetry from the power couplers was largely removed by a special mounting scheme implemented twenty years ago. Local survey errors in the linac sections have been discovered and corrected where the beams are most sensitive. Finally, the irises of the accelerator structure were observed to be tilted slightly about a transverse axis on some accelerator sections.[20] See Fig. 14. The mean tilt angle measured over many sections is zero, but large tilts have been found on certain sections. The cause is most likely angles introduced during the ring brazing technique used during manufacture. The accelerator sections in the region where the beams are most sensitive have been measured and the worst sections removed and replaced with superior units.

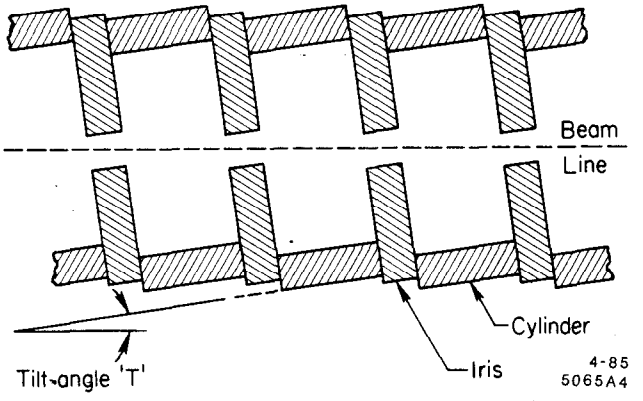

Fig. 14. Observed iris tilting in the SLAC accelerator. Tilt angles can exceed 0.5 mrad (exaggerated in the figure).

TRANSVERSE FEEDBACK SYSTEM:

The transverse feedback system for the SLC linac is schematically shown in Fig. 15. Sensors in Sector 30 near the end of the linac are used to monitor the enlargements of the beams (x, x', y, y' for two beams). A stand-alone microcomputer reads the data, calculates corrections, and sends changes to eight fast dipoles in the ring-to-linac transport lines. The beam signals indicating emittance growth are largest at the end of the linac, but the launching errors must be corrected at the beginning where the beams are most sensitive. The initial complement of sensors will be off-axis profile monitors onto which the SLC beams will be kicked occasionally and the sizes digitized. Beam centroid shifts will also be measured. A fluorescent tail intercepting monitor and a (4×) more sensitive beam position detector will be tested, with hopes that a full repetition rate feedback system can ultimately be made.

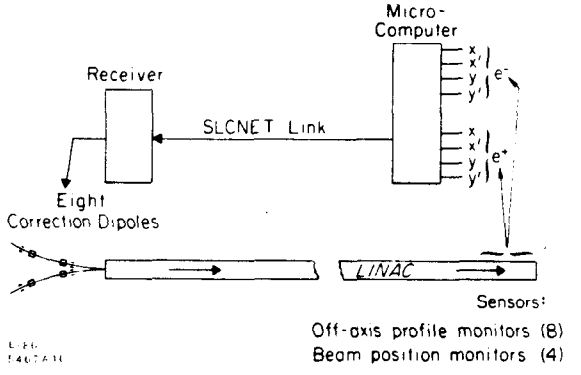

Fig. 15. Transverse feedback system for the linac.

5. Schedules and Plans

The installation of all the equipment for the first 80% of the linac was completed in May 1986. A straight-ahead undamped electron beam has been accelerated through the linac and has been supplied to several experiments. The remainder of the linac will be upgraded in July and August. After an SLC beam is established, the transverse position and the energy feedback systems will be commissioned in September and October 1986. In six to twelve months we expect to have many of the experimental answers on which we can make sound predictions for linacs for future linear colliders.

Acknowledgments

Many people from the SLAC Departments of Accelerator Physics, Electronics, Instrumentation and Control, Mechanical Engineering, Operations, RF and Klystrons, and Software and Modeling have contributed greatly to the upgrade of the SLC linac. K. Bane, M. Ross and R. Stiening are specially recognized for their many contributions.

References

1. J. Sheppard *et al., Proc. of 1984 Linac Accelerator Conf., Darmstadt, W. Germany, GSI-84-11,* 439 (1984).
2. J. Seeman *et al., IEEE* **NS-32, No. 5** *(Vancouver),* 1662 (1985).
3. Z. D. Farkas, *IXth Int. Conf. on High Energy Accelerators, May 1974,* p. 576.
4. M. Allen *et al., 1986 Linear Accelerator Conf., SLAC.*
5. H. Schwarz, *IEEE* **NS-32, No. 5** *(Vancouver),* 1847 (1985)
6. K. Bane and P. Wilson, *XIth Int. Conf. on High Energy Accelerators, Geneva, 1980,* p. 592.
7. SLC Beam Dynamics Task Force, private communication.
8. J. Denard *et al., IEEE* **NS-30, No. 4** *(Sante Fe),* 2364 (1983).
9. J. Seeman *et al., SLC Energy Spectrum Monitor Using Synchrotron Radiation, 1986 Linac Conf., SLAC,* also SLAC-PUB-3945.
10. A. Chao, B. Richter and C. Yao, *Nucl. Instrum. Methods* **178**, 1 (1980), and K. Bane, private communication.
11. J. Bogart *et al., IEEE* **NS-32, No. 5** *(Vancouver),* 2101 (1985).
12. J. Sheppard *et al., IEEE* **NS-32, No. 5** *(Vancouver),* 2180 (1985).
13. M. Ross *et al., IEEE* **NS-32, No. 5** *(Vancouver),* 2003 (1985).
14. V. Balakin *et al., XIIth Int. Conf. on High Energy Accelerators, Fermilab, 1983* p. 119.
15. K. Bane, *IEEE* **NS-32, No. 5** *(Vancouver),* 2389 (1985).
16. J. Sheppard, SLAC Report CN-298 (1985).
17. G. Fischer *et al., XIIth Int. Conf. on High Energy Accelerators, Fermilab, 1983,* p.37.
18. J. Seeman, SLAC Report CN-330 (1986).
19. J. Seeman *et al., IEEE* **NS-32, No. 5** *(Vancouver),* 2629 (1985).
20. J. Seeman, SLAC Report CN-292 (1985).